Molecular Biology of the Cell
Vol. 21, 1648–1661, May 15, 2010

MLT-10 Defines a Family of DUF644 and Proline-rich Repeat Proteins Involved in the Molting Cycle of *Caenorhabditis elegans*

Vijaykumar S. Meli,* Beatriz Osuna,* Gary Ruvkun,† and Alison R. Frand*

*Department of Biological Chemistry, David Geffen School of Medicine, University of California, Los Angeles, Los Angeles, CA 90095-1737; and †Department of Genetics, Harvard Medical School and Department of Molecular Biology, Massachusetts General Hospital, Boston, MA 02114

Submitted July 10, 2008; Revised March 15, 2010; Accepted March 17, 2010
Monitoring Editor: Josephine C. Adams

The molting cycle of nematodes involves the periodic synthesis and removal of a collagen-rich exoskeleton, but the underlying molecular mechanisms are not well understood. Here, we describe the *mlt-10* gene of *Caenorhabditis elegans*, which emerged from a genetic screen for molting-defective mutants sensitized by low cholesterol. MLT-10 defines a large family of nematode-specific proteins comprised of DUF644 and tandem P-X_2-L-(S/T)-P repeats. Conserved nuclear hormone receptors promote expression of the *mlt-10* gene in the hypodermis whenever the exoskeleton is remade. Further, a MLT-10::mCherry fusion protein is released from the hypodermis to the surrounding matrices and fluids during molting. The fusion protein is also detected in strands near the surface of animals. Both loss-of-function and gain-of-function mutations of *mlt-10* impede the removal of old cuticles. However, the substitution mutation *mlt-10(mg364)*, which disrupts the proline-rich repeats, causes the most severe phenotype. Mutations of *mlt-10* are also associated with abnormalities in the exoskeleton and improper development of the epidermis. Thus, *mlt-10* encodes a secreted protein involved in three distinct but interconnected aspects of the molting cycle. We propose that the molting cycle of *C. elegans* involves the dynamic assembly and disassembly of MLT-10 and possibly the paralogs of MLT-10.

INTRODUCTION

The molting cycle is the hallmark of the ecdysozoan clade that encompasses more than 90% of animal species on earth (Aguinaldo *et al.*, 1997). Molting of nematodes involves the synthesis and removal of collagen-rich extracellular matrices (ECM) and related points of cell–ECM adhesion. However, the signaling and enzymatic cascades that trigger and execute the molting process are not well understood. Dysfunction of related processes in humans contributes to the metastasis of tumors and various disorders of skin, connective tissue, and ectodermal organs. These disorders include genetic collagenopathies, certain muscular dystrophies, Marfan syndrome, and baldness (Campbell, 1995; Krause and Foitzik, 2006; Page-McCaw *et al.*, 2007; Blank and Boskey, 2008; Ramirez and Dietz, 2009).

The exoskeleton of nematodes, also called the cuticle, is a complex, multilayered ECM secreted by underlying epidermal-like cells and syncytia (Page and Johnstone, 2007). Collagens serve as major structural components of the cuticle, along with nematode-specific proteins called cuticulins (Cox *et al.*, 1981; Johnstone, 1994; Sapio *et al.*, 2005). Consequently, the *Caenorhabditis elegans* model has been very useful for studies of collagen biosynthesis (Page and Johnstone, 2007). Less is known about the biogenesis of other cuticle components, including the glycoproteins and lipids found in the surface coat and epicuticle, respectively.

During the process of molting, a new cuticle is synthesized underneath the old one and gradually displaces the preexisting structure from the hypodermis. The outer layer of the cuticle is secreted first, and the annular furrows found there correspond to transient invaginations in the apical membrane of the hypodermis (Page and Johnstone, 2007). Particular macromolecules are depleted from the old cuticle during the process of molting, and some scavenged components may, in principle, be incorporated into the new exoskeleton. Lateral attachments that anchor the cuticle to the underlying muscle basement membrane (BM) are also remade during molting.

Larvae eventually escape (ecdyse) from the old cuticle using a stereotypical set of behaviors. This sequence includes regurgitation of the anterior half of the pharyngeal cuticle, rotation on the long axis, contractions, and forward thrusts, in that order (Singh and Soulston, 1978). *C. elegans* larvae molt four times, once every 8–10 h under standard culture conditions. Molting takes about 2 h, but ecdysis takes only a few minutes.

The rapid molting cycle of *C. elegans* requires precise temporal and spatial control over the production and destruction of ECM macromolecules. Accordingly, many genes required for the completion of molting encode proteases and antiproteases involved in the synthesis or degradation of collagens and other ECM proteins (Hashmi *et al.*, 2002, 2004; Davis *et al.*, 2004; Suzuki *et al.*, 2004; Frand *et al.*, 2005; Page

This article was published online ahead of print in *MBoC in Press* (http://www.molbiolcell.org/cgi/doi/10.1091/mbc.E08–07–0708) on March 24, 2010.

Address correspondence to: Alison R. Frand (afrand@mednet.ucla.edu).

Abbreviations used: DUF, domain of unknown function; ECM, extracellular matrix; GFP, green fluorescent protein; GOF, gain-of-function; LOF, loss-of-function; Mlt, molting-defective; NGM, nematode growth medium; NHR, nuclear hormone receptor; RNAi, RNA-interference; WGA, wheat germ agglutinin.

et al., 2006; Partridge *et al.*, 2008). Several genes in the general pathways for secretion and endocytosis are also required for shedding larval cuticles (Roberts *et al.*, 2003; Frand *et al.*, 2005; Roudier *et al.*, 2005). However, the molecular mechanisms that coordinate the assembly and disassembly of extracellular matrices with the progression through ecdysis are not well understood.

The *C. elegans* nuclear hormone receptors NHR-23 and -25 are also required for the removal of larval cuticles (Kostrouchova *et al.*, 1998; Asahina *et al.*, 2000; Gissendanner and Sluder, 2000; Kostrouchova *et al.*, 2001). NHR-23 and -25 are homologous to the ecdysone-responsive DHR3 and FTZ-F1 factors of *Drosophila melanogaster* and also the ROR/RZR/RevErb and SF-1 receptors of mammals, respectively. The requirement for NHR-23 and -25 suggests that steroid hormones regulate the molting cycle of nematodes, similar to how pulses of the steroid hormone ecdysone trigger molting and metamorphosis in insects (Thummel, 1996). NHR-23 and -25 are expressed in hypodermal cells and syncytia and regulate the expression of particular cuticle collagens and matrix modification enzymes (Kostrouchova *et al.*, 2001; Davis *et al.*, 2004; Chen *et al.*, 2004; Silhankova *et al.*, 2005). However, the targets of these receptors germane to the molting cycle have not been fully described in any system (Ruaud *et al.*, 2010).

Large gene families whose members function synergistically were likely to evade detection in any previous RNAi-based screens for molting-defective larvae (Frand *et al.*, 2005). We therefore conducted a forward genetic screen for mutants unable to fully shed old cuticles. Here, we describe the isolation and characterization of the *C. elegans mlt-10* gene, which defines a large family of proteins involved in the episodic synthesis and removal of cuticles during postembryonic development.

MATERIALS AND METHODS

Genetic Analysis

The culture and genetic manipulation of *C. elegans* were performed using standard methods (Epstein and Shakes, 1995). Low-cholesterol (LC) nematode growth medium (NGM) was prepared with SeaKem GTG agarose (FMC, Rockland, ME) rather than agar and no added cholesterol. *Escherichia coli* OP50 were washed with M9 buffer before seeding LC plates. Bacterial-mediated RNA-interference (RNAi) was performed as described (Fraser *et al.*, 2000), except that NGM was supplemented with 8 mM IPTG and 25 μg/ml carbenicillin. Table S1 describes the *C. elegans* strains used in this study.

To isolate mutants more sensitive to low cholesterol, GR1462 was mutagenized with ethylmethane sulfonate (EMS, Sigma, St. Louis, MO). About 15,000 embryos from the first filial (F_1) generation were collected and cultured on NGM. Hatchlings from the second filial (F_2) generation were collected and cultured on LCNGM at a density of roughly 200 animals per 6-cm plate. After 3 d, 664 larvae that had arrested at the L1 or L2 stage were individually transferred to NGM plates and 71 thereafter developed into adults and produced progeny. Descendents of those 71 animals were retested for growth on LCNGM. Monitoring expression of the *dpy-7p::gfp* reporter gene present in GR1462 enabled simultaneous screening for mutants defective in NHR-23 signaling.

The *mlt-10(mg364)* mutant was typically cultured on bacteria expressing *mlt-10* double-strand RNA (dsRNA) and subsequently was fed OP50 for two generations before phenotypic analysis. To isolate intragenic suppressors, *mlt-10(mg364RNAi)* animals were mutagenized with EMS. Approximately 20,000 F_1 animals were collected and fed OP50 on NGM. The F_2 hatchlings were then collected and cultured at a density of 50 animals per 6-cm plate. Rare plates on which the F_2 and F_3 animals rapidly consumed all of the available food were identified. Picking a single worm from each plate led to the isolation of 44 suppressed lines. To test for linkage between a particular suppressor and *mlt-10*, the strain was out-crossed to KP3913 (*nuIs163*[*myo-2p::gfp*] II), and the F_2 animals were observed for molting defects. We reiteratively out-crossed *mlt-10(mg416mg364)* animals to KP3913 to separate the two mutations in *mlt-10*. The *mlt-10(ok2581)*, *mlt-10(cxTi9515)*, and *mlt-10(tm3331)* mutations were out-crossed to KP3913 to generate ARF202, ARF201, and ARF204, respectively. Notably, we observed immobility and lethality in adults of the original *mlt-10(ok2581)* strain RB1962 but not the out-crossed strain ARF202.

The arrays *mgEx701* and *mgEx699* were made by microinjection of *mlt-10(mg364)* (5 ng/μl) or *mlt-10* (10 ng/μl) DNA, respectively, along with a *sur-5::gfp* plasmid (50 ng/μl; Yochem *et al.*, 1998) and pBS (40 ng/μl) into wild-type adults. To ameliorate the toxicity associated with increased dosage of *mlt-10*, transgenic nematodes were cultured on bacteria expressing *mlt-10* dsRNA. Similar methods were used to make arrays containing *mltn-4*/W02B8.4 and *mltn-7*/Y39D8B.1. To generate *aaaEx16*, the *mlt-10::mCherry* plasmid (5 ng/μl) was microinjected into *pha-1(e2123)* animals along with the *pha-1(+)* plasmid pBX (5 ng/μl), the *myo-2p::gfp* plasmid pPD118.33 (10 ng/μl), and pBS (80 ng/μl). To generate *aaaEx19*, the *gfp::mlt-10* plasmid (10 ng/μl) was microinjected into N2 animals along with pBS (80 ng/μl) and a *myo-2p::rfp* plasmid (10 ng/μl) provided by Cheryl Van Buskirk (California Institute of Technology).

Molecular Biology

Table S2 lists the sequence of PCR primers used in this study. To sequence *mlt-10/C09E8.3*, genomic DNA was amplified from worm extracts and sequenced using primers AFP6 through AFP31. To genotype *tm3331*, *ok2581*, and *cxTi9515*, genomic DNA was amplified with primer sets AFP15/AFP26, AFP46/AFP31, and AFP45/AFP23, respectively. Genomic DNA was amplified from RB1962, cloned into pCR-XL-TOPO (Invitrogen, Carlsbad, CA), and sequenced to determine the expanse of the *ok2581* lesion. Toward the production of high-copy arrays, *mlt-10* was amplified from genomic DNA using primers AFP1 and AFP3 and the Expand Long Template PCR kit (Roche, Indianapolis, IN). The *mltn-4*/W02B8.4 and *mltn-7*/Y39D8B.1 genes were amplified from genomic DNA using primer sets AFP41/AFP42 and AFP43/AFP44, respectively. Toward RNAi of *mltn-10*/F19H8.5, *mltn-1*/F32A11.7, *mltn-5*/W02B8.6, and *mltn-7*/Y39D8B.1, genomic DNA was amplified using primer sets AFP32/AFP33, AFP34/AFP35, AFP36/AFP37, and AFP38/AFP39, respectively. Each PCR product was cloned into pCR-XL-TOPO and subsequently into pPD129.36 (Fire Lab, Stanford University School of Medicine) and *E. coli* strain HT115(DE3).

The *mlt-10p::gfp-pest* fusion gene was generated as previously described (Frand *et al.*, 2005). To construct translational fusion genes, the *mlt-10* gene and regulatory sequences were amplified from N2 genomic DNA using primers AFP47 and AFP48 and Phusion High-Fidelity Polymerase (Finnzymes). The PCR product was cloned into pCR-Blunt II-TOPO (Invitrogen). The NotI site in the vector was filled using Klenow (NEB, Ipswich, MA). The resulting plasmid (pAF599) contained a single C to A transition, at the base corresponding to nucleotide 10407 of cosmid C09E8. A new NotI site was generated in pAF599 using the Phusion Site-Directed Mutagenesis kit (Finnzymes, Espoo, Finland) with primers AFP49 and AFP50. The site was inserted in-frame between the last coding codon and the stop codon of *mlt-10*. A NotI cassette containing the *mCherry* gene was cloned into the resulting vector from KP1272 (a gift from Lars Drier, University of California, Los Angeles). Separately, an NotI site was generated in pAF599 in-frame between the codons specifying Ala30 and Val31 of MLT-10. An NotI cassette containing the *gfp* gene was isolated from pPD114.35 (Fire Lab) and cloned into the resulting vector.

RNA was isolated from *C. elegans* as described (Pasquinelli *et al.*, 2000). We used the TURBO kit (Ambion, Austin, TX) to remove any contaminating genomic DNA and the RETROscript kit (Ambion) with random primers to synthesize cDNA. The *mlt-10* cDNAs were amplified using primers sets AFP14/AFP27 or AFP15/AFP30. The *ama-1* cDNAs were amplified using primers *ama-1*-262 and *ama-1*-263, kindly provided by Eyleen O'Rourke (Harvard Medical School). PCR products were separated by agarose-gel electrophoresis and stained with ethidium bromide.

Microscopy and Cell Biology

Nematodes were anesthetized using sodium azide and mounted on 2% agarose pads. Images were captured using a Zeiss Axioscope (Thornwood, NY) with an attached Hamamatsu Orca ER camera (Bridgewater, NJ) and Volocity software (Improvision, Lexington, MA). For confocal work, we used a Zeiss LSM 5 PASCAL microscope and Axiovision software (Zeiss). All images were prepared for publication using Adobe Photoshop and Adobe Illustrator (San Jose, CA).

Larvae were stained with Hoechst 33258 (Sigma) as previously described (Moribe *et al.*, 2004). To detect surface glycans, animals were incubated in M9 buffer containing 50 μg/ml WGA-Alexa Fluor 488 (Invitrogen) for 40 min with gentle agitation at room temperature. Samples were washed in M9 three times to remove unbound WGA.

RESULTS

Isolation of mlt-10 in a Forward Genetic Screen

Nematodes cannot synthesize cholesterol de novo (Hieb, 1968; Chitwood, 1999). *C. elegans* must therefore acquire sterols from the culture medium in order to produce various steroid hormones essential for development and reproduction (Crowder *et al.*, 2001; Merris *et al.*, 2003; Matyash *et al.*, 2004; Motola *et al.*, 2006). Wild-type larvae cultured without

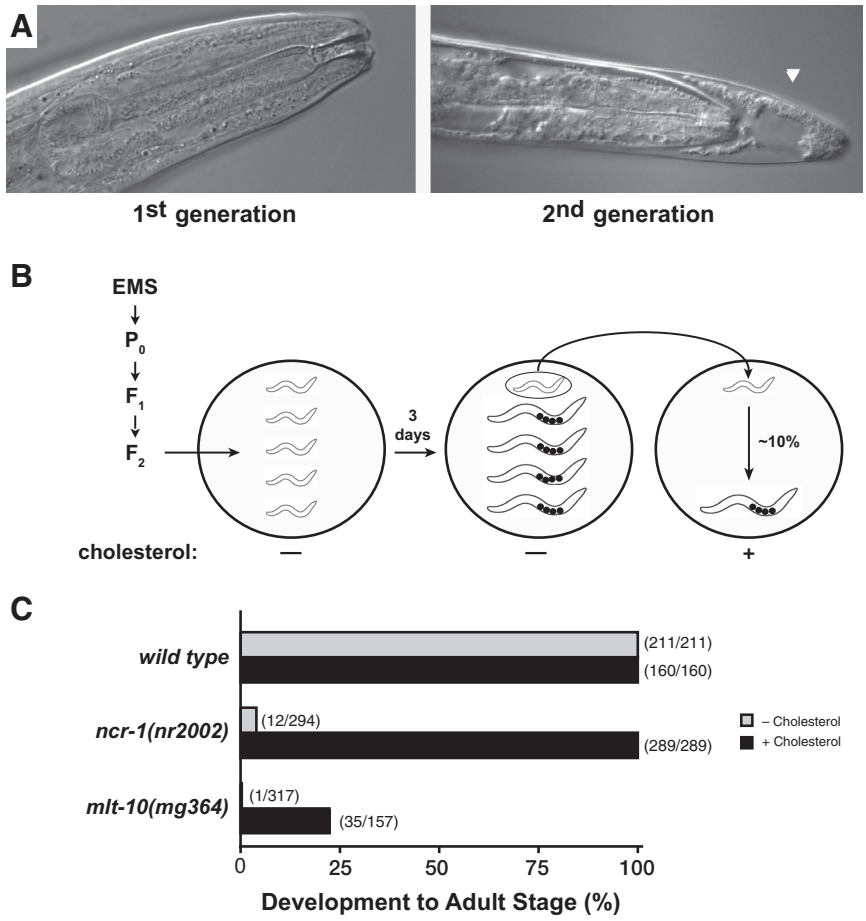

Figure 1. Genetic screen for mutants more sensitive to low cholesterol. (A) Representative Nomarski micrographs of *C. elegans* grown on LCNGM for one or two generations. Left, an adult; right, a larva trapped in partly shed cuticle (arrowhead). (B) Design of the screen. (C) Growth of L1 larvae to the adult stage on LCNGM (gray) or NGM (black) after cultivation for 5 d at 20°C. Parents of the observed animals were cultured on NGM.

cholesterol can rely on sterols stored by their mothers to develop to the adult stage. However, the progeny of animals cultured on low-cholesterol media arrest development as larvae, often trapped in partly shed cuticle: the *molt*ing-defective or Mlt phenotype (Figure 1A: Yochem *et al.*, 1999). We used low cholesterol to sensitize a forward genetic screen for mutants unable to fully shed old cuticles (Figure 1B). Briefly, we isolated 17 mutants that require exogenous cholesterol, in addition to any maternal stores of cholesterol, to complete larval development. Larvae descended from 13 of the 17 mutants showed the Mlt phenotype under standard culture conditions (data not shown).

The *mg364* allele of *mlt-10* emerged from our screen. We analyzed the phenotypes associated with *mg364* after outcrossing several times to remove any unlinked mutations. Only 0.3% (n = 317) of *mlt-10(mg364)* larvae developed to the adult stage when cultured on low-cholesterol media, compared with 100% (n = 211) of wild-type larvae (Figure 1C). As previously reported, mutations in the *C. elegans ncr-1* gene also blocked development on low-cholesterol plates (Sym *et al.*, 2000; Li *et al.*, 2004). The *ncr-1* gene is homologous to the human Niemann-Pick type C1 disease gene, which is important for the proper transport and storage of cholesterol (Smith and Levitan, 2007).

Under standard culture conditions, 56% (n = 466) of homozygous *mlt-10(mg364)* animals became trapped in a larval cuticle (Figure 2A). Roughly the same fraction of animals became trapped in each one of the four molts. Larvae incarcerated in a molt typically perished. An additional 22% of *mg364* larvae arrested development but did not appear trapped in the cuticle upon inspection by light microscopy. The surviving *mg364* animals developed slowly, with a generation time of ~90 h at 20°C, compared with 65 h for wild-type animals. The Mlt phenotype was also observed in 16% (n = 365) of heterozygous *mlt-10(mg364)/mlt-10(+)* animals, indicating that *mg364* is semidominant. Together, these results show that *mlt-10(mg364)* causes a strict blockade of the molting cycle.

The mlt-10 Gene Corresponds to C09E8.3

To identify the *mlt-10* gene, we mapped the *mg364* mutation to a 3.4 map unit region on the left end of chromosome II by standard methods (Wicks *et al.*, 2001). Because the *mg364* mutation was semidominant, we reasoned that inactivation of *mlt-10* might restore the ability of *mg364* mutants to shed old cuticles. We therefore systematically and individually inactivated the annotated genes in the map interval by bacterial-mediated RNAi (Timmons *et al.*, 2001; Kamath *et al.*, 2003). After the inactivation of C09E8.3, the vast majority of *mlt-10(mg364)* larvae developed into healthy adults (Figure 2B). Sequencing C09E8.3 identified a C-to-T transition in *mg364* mutants that specifies the substitution H590Y in the predicted MLT-10 protein. In addition, an extrachromosomal array containing C09E8.3 amplified from *mg364* mutants (*mgEx701*, Figure S1) rendered wild-type larvae unable to shed old cuticles. To confirm the identity of the gene, we isolated and characterized six additional alleles of *mlt-10* by screening for intragenic suppressors of *mg364*. The new alleles included four distinct missense mutations and two splice-site mutations in C09E8.3 (Table S3). Together, these

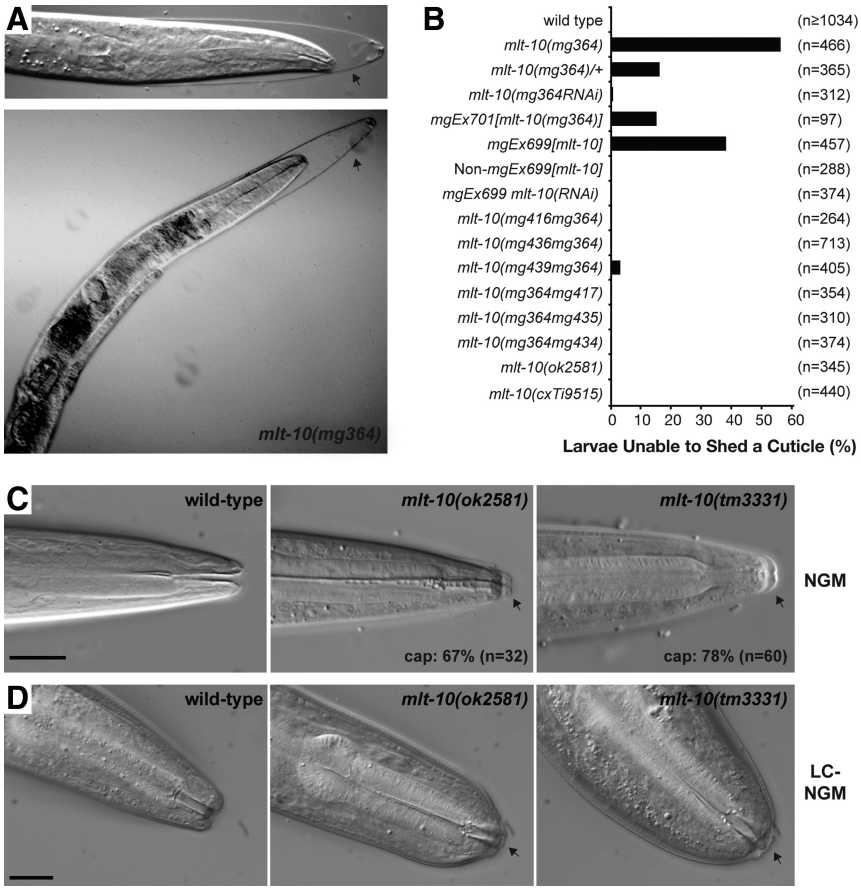

Figure 2. Mutations of *mlt-10* hinder the removal of larval cuticles. (A) Representative Nomarski micrographs of *mlt-10(mg364)* mutants. Top, a midstage larva; bottom, an adult encased in the L4-stage cuticle (arrow). (B) Animals of each genotype were collected as embryos, cultured on NGM for 3–5 d at 20°C, and inspected using a dissecting microscope. Graph shows the percent of animals trapped in a larval cuticle. Not all genotypes were tested concurrently. (C and D) Representative Nomarski micrographs show animals of the indicated genotypes. (C) Animals were collected as embryos, cultured on NGM for 45 h at 20°C, and inspected using a compound microscope. Arrows indicate the buccal caps. (D) Hatchlings were collected and cultured on LCNGM for 3 d at 20°C. Arrows indicate unshed cuticles from the L4 larval stage. Scale bars, 10 μm.

results show that *mlt-10* corresponds to C09E8.3 and that *mg364* is a gain-of-function (GOF) allele.

Figure 3A shows the structure of the *mlt-10* gene, as confirmed by the sequence of 76 distinct cDNAs curated by Wormbase (www.wormbase.org). In addition to the point mutations described above, we obtained a variety of *mlt-10* alleles from public resources. These alleles included *cxTi9515*, *tm3331*, and *ok2581*, reagents kindly provided by Laurent Segalat (University of Lyon), the *C. elegans* Gene Knockout Consortium, and the National Bioresource Project of Japan, respectively (Table S3). The *cxTi9515* allele is an insertion of the *Mos1* transposon in the 5′ UTR of *mlt-10* (Bessereau *et al.*, 2001; Martin *et al.*, 2002). The mutation severely decreased the level of *mlt-10* expression, as indicated by RT-PCR (Figure S2). The *mlt-10(tm3331)* insertion/deletion causes a frame-shift in exon 3 that introduces an early stop codon. The *ok2581* insertion/deletion encompasses exons 5 through 7 and part of exon 8. Transcripts of *mlt-10* were shorter and less abundant in *ok2581* mutants than wild-type animals (Figure S2). Sequencing those cDNAs indicated the use of an atypical splice acceptor site for exon 8 and the related introduction of a premature stop codon. As we shall describe, we analyzed the phenotypes associated with these loss-of-function (LOF) alleles of *mlt-10* after out-crossing the corresponding strains several times to remove any unlinked mutations.

MLT-10 Defines a Family of DUF644 and Proline-rich Repeat Proteins

MLT-10 is the first characterized member of a large family of annotated proteins comprised of the domain of unknown function (DUF) 644 and distinctive tandem repeats rich in prolines and hydroxy amino acids (Figure 3, B and C, Figures S3 and S4). DUF644 contains many lysine residues and other basic or acidic amino acids. The repeats found at the C-terminus of MLT-10 have the consensus sequence P-X_2-L-(S/T)-P, where X is any hydrophobic residue except glycine. MLT-10 also contains an annotated secretory signal sequence and four putative acceptor sites for N-linked glycans, features characteristic of secreted proteins.

In principle, the biosynthesis of MLT-10 and the paralogs of MLT-10 may involve several posttranslational modifications, including but not limited to 1) disulfide bond formation, 2) the addition of O-linked glycans, 3) cleavage of dibasic sites in the nonrepetitive region by subtilisin/Kex2-like proteases, 4) cross-linking of glutamine and lysine residues by transglutaminase, and 5) the hydroxylation of some proline residues in the repetitive region. These particular modifications occur during the biosynthesis of collagens and other ECM proteins of nematodes (Fetterer and Rhoads, 1990; Lustigman *et al.*, 1995; Thacker and Rose, 2000; Edens *et al.*, 2001; Page *et al.*, 2006).

We identified 13 paralogs of *mlt-10* in the fully sequenced genome of *C. elegans* and named those genes *mltn-1* through *mltn-13* for (mlt-ten-related; Figure 3C and Table S4). Previous high-throughput analysis indicated that most if not all of the *C. elegans mltn* genes are expressed (Wormbase). The MLT-10 paralogs include *mltn-1*/F32A11.7, *mltn-2*/Y52B11A.7, *mltn-11*/W06G6.7, *mltn-12*/C53B4.8, and *mltn-13*/F15A8.7, as well as three genes on cosmid W02B8 (II:13,916,260–13,930,421), two genes on cosmid F19H8 (II:14,616,033–14,626,346), and three genes on cosmid Y39D8B (V:364,951–379,673). Nota-

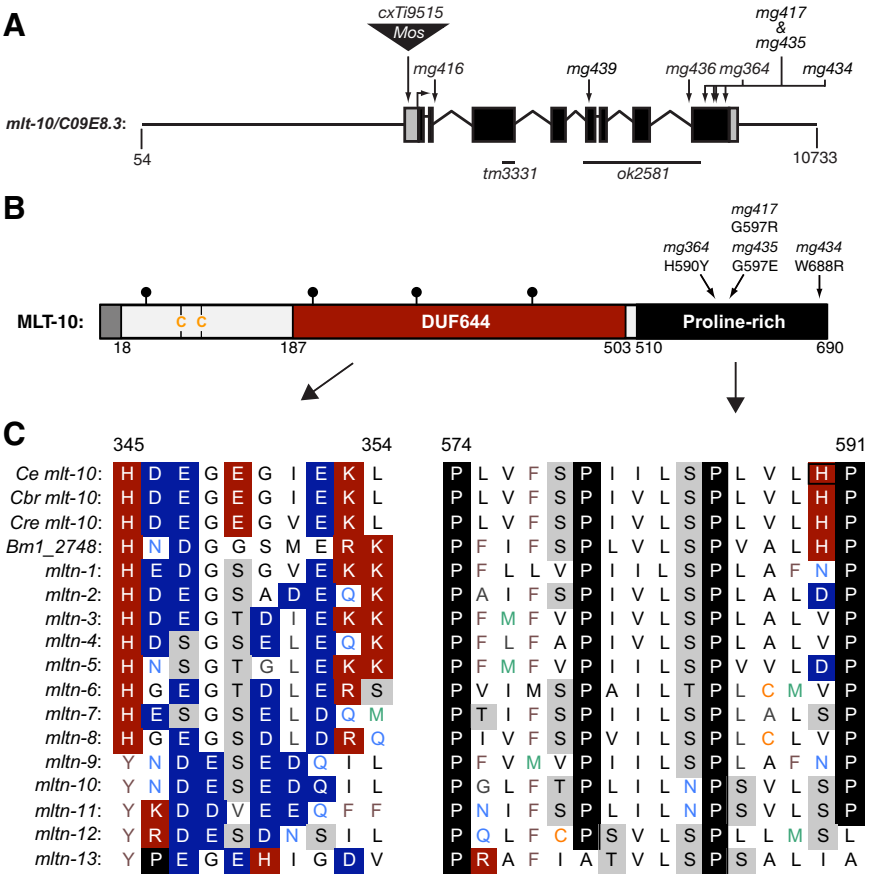

Figure 3. MLT-10 defines a large family of nematode-specific proteins. (A) Diagram of the *C. elegans mlt-10* gene and flanking sequences. Black boxes represent exons, and gray boxes represent untranslated sequences. Nucleotide positions correspond to cosmid C09E8 (Accession no. gb AF077529). Table S3 further describes these mutations of *mlt-10*. (B) Diagram of the predicted MLT-10 protein (Accession no. gi 17531703) showing the signal sequence (gray), potential acceptor sites for N-linked glycans (●), conserved cysteine residues; DUF644 (red), and the proline-rich region (black). (C) Sequence alignment of the predicted paralogs and selected orthologues of MLT-10. Amino acid positions correspond to *Ce* MLT-10. Acidic and basic residues are shaded blue and red, respectively. Prolines are shaded black and hydroxy amino acids are shaded gray. The H590 residue affected by *mg364* is boxed. Accession numbers for these sequences are *Ce*, ref NM_061354; *Cbr*, gi 187040316; *Cre*, gi 183180662; and *Bm1_2748*, gi 170584318. Table S4 provides additional information about the *mltn* genes of *C. elegans*.

bly, several of the gene models described in Table S4 include exons not depicted in the current release of Wormbase (WS204). In particular, the gene annotated as Y39D8B.1 in WS204 represents an in silico fusion of the predicted paralogs *mltn-6* and *mltn-7*, formerly annotated as Y39D8B.2 and Y39D8B.1, respectively, in WS100. The fused gene depicted in WS204 specifies an atypical protein containing two copies of DUF644 but only one set of proline-rich repeats. The existence of three clusters of paralogs in the genome suggests that multiple gene duplication events contributed to evolution of the *mlt-10* family. Many homologues of MLT-10 were also identified in the genomes of other species of nematodes and the annotated proteomes of parasitic nematodes including *Onchocerca volvulus* and *Brugia malayi*, which cause River Blindness and lymphatic filariasis in humans, respectively (Figure 3C and S4).

Figure S4 displays an alignment of the P-X_2-L-(S/T)-P repeats of the predicted paralogs and selected homologues of MLT-10. Most of these proteins contain about 30 repeats interspersed with only a few charged residues, with the exception of MLTN-13/F15A8.7. Repeats similar to those of MLT-10 were found in several annotated but uncharacterized and otherwise unrelated proteins of eukaryotes, suggesting a widespread and ancient function for the [P-X_2-L-(S/T)-P]$_n$ sequence. We identified such proteins in the translated genomes of *Xenopus laevis* (gi 47125144), *Tetraodon nigroviridis* (gi 47221831), *Homo sapiens* (ref NW_001837930: 1954604–1955196), and *Candida tropicalis* (gi 255731458). A similar P-X_4-P sequence also occurs in the *Bordetella pertussis* virulence factor Pertactin (gi 6730300; Emsley *et al.*, 1996). Proteins with DUF644 were not readily identified by standard TblastN searches (Altschul *et al.*, 1990) of the fully sequenced genomes of *D. melanogaster*, *H. sapiens*, or *Saccharomyces cerevisiae*. Thus, MLT-10 defines a large family of proteins that is well conserved only in nematodes.

Either the Loss or the Gain of mlt-10 Function Hinders the Removal of Larval Cuticles

We used genetic analysis to investigate the role of the *mlt-10* family in development and better define the nature of the *mlt-10(mg364)* allele. A variety of *mlt-10(lof)* mutants developed from the L1 to the adult stage more slowly than wild-type animals, but did not display a terminal Mlt phenotype (Figure 2B). We therefore closely examined larvae partially synchronized around the time of the L2-to-L3 molt, using a compound microscope to detect buccal caps. The caps are comprised of old cuticle and temporarily seal the buccal cavity during the process of molting. Caps were observed on the majority of *mlt-10(tm3331)* and *mlt-10(ok2581)* mutants (Figure 2C), compared with 20% (n = 76) of wild-type larvae. When cultured on low-cholesterol media, 70% (n = 13) of *mlt-10(tm3331)* mutants and 92% (n = 12) of *mlt-10(ok2581)* mutants failed to shed the fourth larval cuticle, compared with 29% (n = 14) of wild-type animals (Figure 2D). Together, these results suggest that *mlt-10* is needed for the efficient removal of larval cuticles, even though *mlt-10* is not essential for development under standard culture conditions.

To further evaluate the function of the *mlt-10* family, we used RNAi to systematically and individually knock down the 13 annotated paralogs of *mlt-10* in wild-type larvae; *mlt-10(lof)* mutants; and *rrf-3* mutants, which are more sensitive to dsRNA (Simmer *et al.*, 2002). None of these animals became terminally trapped in cuticle (Table S5). Also, the

Mlt phenotype was not associated with *gk766*, a deletion in the *mltn-13*/F15A8.7 gene. Thus, the paralogs of *mlt-10* appear individually dispensable for the removal of larval cuticles, possibly due to functional redundancy among the large gene family. A thorough investigation of any such redundancy awaits the availability of null alleles in all thirteen paralogs of *mlt-10*.

As a complementary approach to investigate the *mlt-10* family, we used high-copy arrays to increase the dosage of *mlt-10* and selected paralogs of *mlt-10.* The array *mgEx699[mlt-10]* rendered 38% (n = 457) of larvae unable to shed old cuticles, and RNAi of *mlt-10* suppressed that phenotype (Figure 2B). As expected, wild-type *mlt-10* appeared less toxic than *mlt-10(mg364)* after the microinjection of equivalent amounts of DNA (data not shown). High-copy arrays that contained *mltn-4* and *mltn-7* also conferred the Mlt phenotype. High-copy arrays that contained *mltn-3* and *mltn-11* caused embryonic and larval lethality prohibitive to the propagation of transgenic nematodes (data not shown). Thus, increased expression of *mlt-10*, *mltn-4*, or *mltn-7* can prevent the removal of larval cuticles. Activities of the other *mltn* genes will be tested in future work.

Our screen for intragenic suppressors of *mlt-10(mg364)* identified additional mutations that affect the proline-rich repeats of MLT-10. As previously stated, *mg364* specifies the substitution H590Y. H590 is conserved among the annotated orthologues of MLT-10 and is one of only five charged residues present in the repetitive region (Figure S4). The intragenic suppressors *mg417*, *mg434,* and *mg435* specified the substitutions G597R, W688R, and G597E, respectively. None of these missense mutations blocked expression of the *mlt-10(mg364)* gene (Figure S2). However, each of the corresponding substitutions introduced a charged residue into the repetitive region. The mechanism of suppression may therefore involve the rectification of MLT-10(H590Y) or destabilization of the otherwise toxic protein. The *mg416* and *mg436* mutations affected splice sites of *mlt-10* and reduced expression of the gene (Figure S2). The sequence of *mlt-10(mg416)* cDNAs indicated correct splicing. In contrast, the sequence of *mlt-10(mg436mg364)* cDNAs indicated the use of an atypical splice acceptor site for exon 8 and the related introduction of a premature stop codon upstream of the proline-rich repeats (Table S3). In this case, diminished expression of the repetitive region likely accounts for the suppression of *mg364*. Taken together, these findings indicate that dysfunction of the repetitive region of MLT-10 blocks the removal of larval cuticles. Moreover, the data suggest that electrostatic interactions involving the P-X_2-L-(S/T)-P repeats influence the utility of MLT-10. As we shall discuss, we hypothesize that MLT-10(H590Y) interferes with the function of multiple members of the MLT-10 family, as does increased expression of wild-type MLT-10.

The mlt-10 Gene Is Expressed in the Hypodermis during Larval Development

To determine the spatial and temporal expression pattern of *mlt-10*, we fused the promoter of *mlt-10* to the *gfp-pest* gene, which encodes a variant of green fluorescent protein (GFP) that is rapidly degraded in vivo (Li *et al.,* 1998; Frand *et al.,* 2005). The *mlt-10p::gfp-pest* fusion gene was expressed in the major body hypodermal syncytium (Hyp7), the dorsal and ventral ridges of the hypodermis, hypodermal cells in the head and tail, and the pharyngeal myoepithelium, but not the lateral seam cells (Figure 4A). In L4-stage animals cultured at 25°C, GFP was first detected in the anterior hypodermis ~3.5 h before ecdysis. The fluorescence spread throughout Hyp7 and intensified for about 3 h. The fluorescence dissipated at the end of lethargus and was barely detectable 1 h after ecdysis (Figure 4A). A similar pulse of expression of GFP accompanied all four molts and faithfully recapitulated expression of the endogenous *mlt-10* gene, as previously described (Frand *et al.,* 2005). GFP was also expressed in epidermal cells of pretzel-stage embryos, which synthesize the cuticle for the first larval stage (data not shown). We conclude that most hypodermal cells and syncytia express *mlt-10* whenever a new exoskeleton is made.

We previously reported that NHR-25 and -23 drive supernumerary bouts of expression of *mlt-10* in *let-7* family mutants that continue molting after the fourth larval stage (Hayes *et al.,* 2006). Here, we asked if *nhr-25* and *-23* also regulate expression of *mlt-10* during larval development. We used RNAi to knockdown *nhr-25* or *-23* in *mgIs49[mlt-10p::gfp-pest]* larvae. The hypomorphic allele *nhr-25(ku217*) was used to sensitize animals to RNAi of *nhr-25* (Chen *et al.,* 2004). Sets of larvae were repeatedly monitored for expression of GFP over an 8-h time period encompassing the L4-to-adult molt. The mid-L4-stage larvae selected for this experiment were active at the start, but became lethargic and attempted to shed the L4-stage cuticle by the end. Only 40% (n = 49) of *nhr-25(ku217RNAi)* animals expressed the GFP reporter during this time, compared with 100% (n = 22) of control animals. Moreover, the fluorescence associated with GFP was dim and ephemeral in *nhr-25(ku217RNAi)* mutants, compared with wild-type animals. None (n = 24) of the *nhr-23(RNAi)* animals expressed any detectable GFP, as previously reported (Frand *et al.,* 2005). RNAi of *nhr-25* or *-23* also greatly reduced the abundance of *mlt-10* messages in late L4 larvae, as indicated by RT-PCR (Figure 4B). Thus, NHR-25 and -23 promote expression of *mlt-10* during the larval molting cycle.

To detect the MLT-10 protein in vivo, we constructed two distinct, full-length translational fusion genes between *mlt-10* and fluorescent reporters (Figure S1). The mCherry tag was inserted at the C-terminus of MLT-10. GFP was inserted downstream of the predicted signal sequence. The corresponding arrays conferred many of the same phenotypes as *mgEx699[mlt-10]*, confirming expression of the MLT-10 fusion proteins.

During the process of molting, the MLT-10::mCherry and GFP::MLT-10 fusion proteins were detected in vesicle-like objects near the apical surface of the epidermis (Figure 5, A and B). Cherry was also readily detected in other structures, whereas GFP was not, possibly due to proteolytic processing of the N-terminal fusion protein.

In young adults, the MLT-10::mCherry fusion protein was also detected in coelomocytes, distinctive scavenger cells that endocytose material from the pseudocoelom (Grant and Sato, 2006). Cherry was detected in the coelomocytes of ~22% (n = 176) of *aaaEx16[mlt-10::mCherry]* animals. Fusion proteins secreted from the apical surface of the hypodermis may have mixed with coelomic fluids in this particular background, because the *mlt-10::mCherry* array was associated with gaps in the syncytial epidermis, as we shall describe. Alternatively, some MLT-10::mCherry may have been released from the basolateral surface of Hyp7 or the pharyngeal myoepithelium. In either case, uptake by coelomocytes verified that MLT-10::mCherry was secreted, as coelomocytes do not express the *mlt-10* gene. Collectively, these observations suggest that MLT-10 is released from the hypodermis to the surrounding matrices and fluids during the process of molting.

The MLT-10::mCherry fusion protein was also detected in strands and loops near the surface of transgenic animals (Figure 5D). These structures were observed in 27% (n = 123) of mixed-stage larvae, but were most prominent in

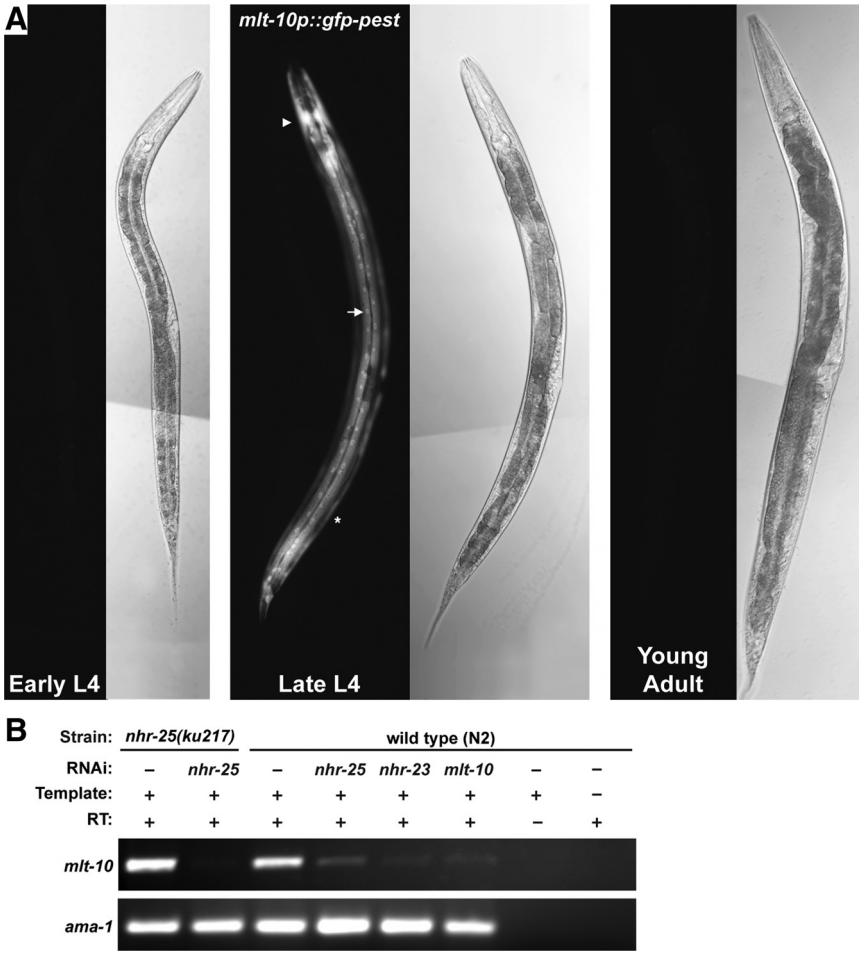

Figure 4. Spatial and temporal expression pattern of *mlt-10.* (A) Representative fluorescence and Nomarski micrographs show expression of the *mlt-10p::gfp-pest* fusion gene. GFP was detected in the major body hypodermal syncytium (arrow), the dorsal and ventral ridges of the hypodermis (asterisk), and the anterior hypodermis (arrowhead) of the late L4 stage larva. All fluorescence images were acquired with an exposure time of 187 ms. (B) Detection of *mlt-10* transcripts by RT-PCR. Larvae were cultured on bacteria that expressed the indicated dsRNAs for 40 h at 25°C. Animals were harvested at the typical time of the L4-to-adult molt. Detection of *ama-1* transcripts controlled for the quality of RNA samples and RT-PCR reactions.

animals completing the fourth molt. The strands ranged from 5 to 30 μm in length and appeared to be positioned above the hypodermis. The formal possibility that these structures result from the nonspecific aggregation of mCherry cannot be eliminated at this time. Nonetheless, these observations are consistent with the model that MLT-10 assembles into oligomeric complexes in vivo. A complete description of any such complexes awaits the availability of anti-MLT-10 antibodies.

Either the Loss or the Gain of mlt-10 Function Impinges on the Exoskeleton

The molting cycle involves both the synthesis and the removal of cuticles, and these processes are likely interconnected. We therefore examined several aspects of the exoskeleton to more fully define the phenotypes associated with particular mutations in *mlt-10.* To determine the effect of MLT-10(H590Y) in the absence of unshed cuticles, we examined *mlt-10(mg416mg364)* double mutants, rather than *mlt-10(mg364)* single mutants, in many experiments.

To evaluate the barrier function of the exoskeleton, we treated larvae with the DNA-binding dye Hoechst 33258, as previously described (Moribe *et al.,* 2004). The *mlt-10(tm3331)*, *mlt-10(ok28581)*, *mlt-10(mg364)*, and *mlt-10(mg416mg364)* mutants were all more permeable to Hoechst than wild-type larvae (Figure 6). In this regard, *mlt-10(mg364)* larvae resembled *bus-8(e2887)* mutants, which have more porous cuticles because of a defect in the glycosylation of secreted proteins (Partridge *et al.,* 2008). The increased permeability of *mlt-10(mg416mg364)* mutants to Hoechst was directly attributable to expression of the MLT-10(H590Y) protein, because *mlt-10(mg416)* single mutants were not permeable to the dye. High-copy *mlt-10(+)* and *mlt-10::mCherry* arrays were also associated with increased permeability of the cuticle (data not shown). As a complementary approach, we tested the ability of animals to survive chronic osmotic stress. The survival rate of various *mlt-10* mutants was significantly lower than that of wild-type animals on media containing 300 mM NaCl (Figure 6F). Thus, mutations of *mlt-10* decrease the utility of the exoskeleton as a barrier to the environment.

To detect a cuticle collagen in vivo, we used a translational fusion gene between *col-19* and *gfp*, kindly provided by Anthony Page (University of Glasgow). In wild-type animals, COL-19::GFP is incorporated into the circumferential annuli and longitudinal alae of the adult exoskeleton (Thein *et al.,* 2003). In contrast, COL-19::GFP macromolecules were disorganized in many *mlt-10(tm3331)* and *mlt-10(ok2581)* animals (Figure 7). Expression of MLT-10(H590Y) or MLT-10::mCherry also interfered with the assembly of COL-19::GFP, particularly above the lateral hypodermis (Figure S5). The severity of disorganization of COL-19::GFP varied among isogenic *mlt-10* mutants, perhaps because of compensatory changes in the expression of other MLTN proteins. We conclude that both LOF and GOF mutations of *mlt-10* affect the patterning of COL-19::GFP and possibly other cuticle collagens.

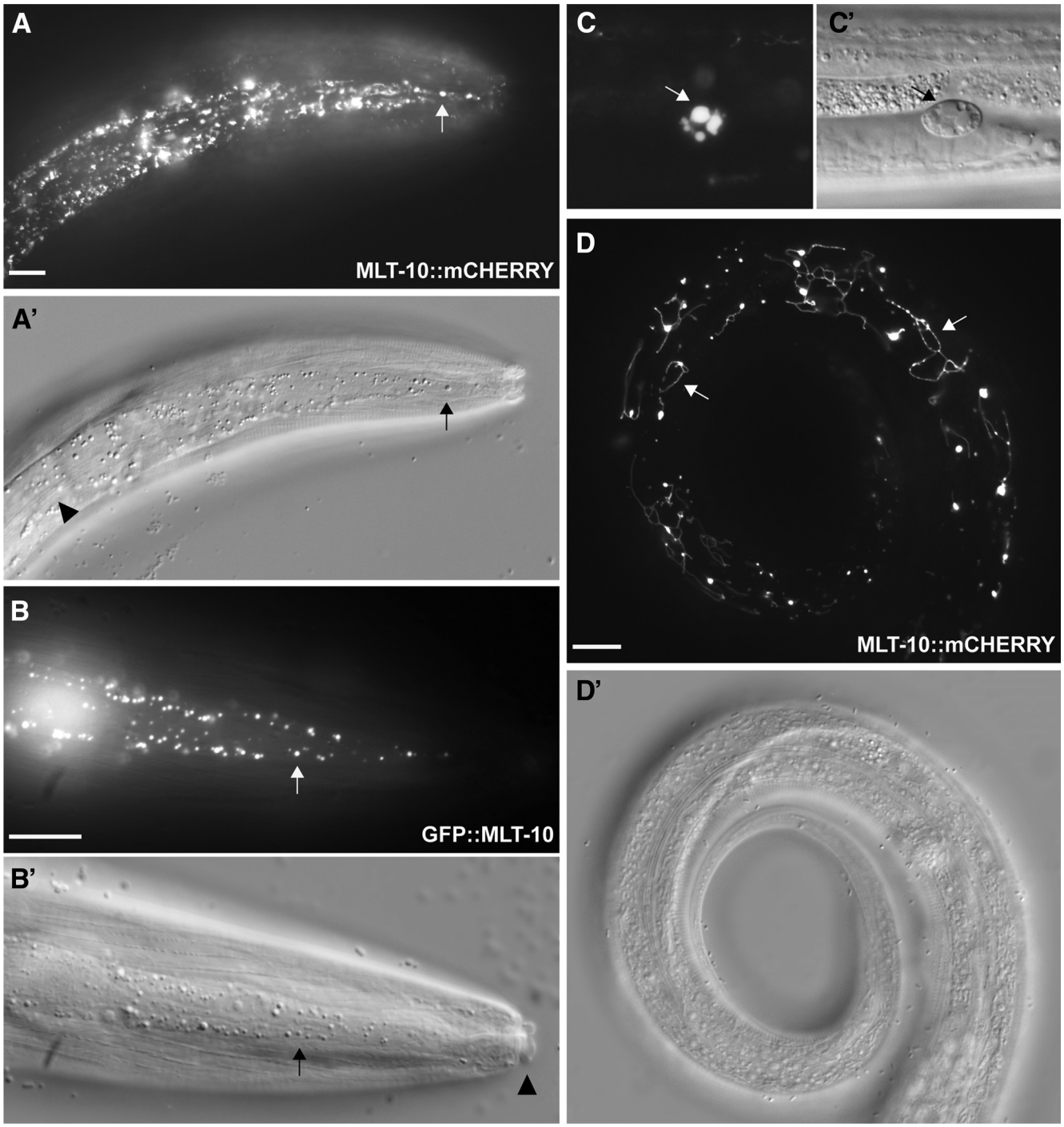

Figure 5. Localization of the MLT-10::mCherry and GFP::MLT-10 fusion proteins. (A–D) Representative fluorescence and Nomarski micrographs show expression of the fusion proteins. (A) MLT-10::mCherry detected in vesicle-like objects (arrow) in the lateral epidermis of a late L4 larva molting to the adult stage. Alae are visible on the underlying cuticle (arrowhead). (B) GFP::MLT-10 detected in vesicles (arrow) in the lateral epidermis of a molting larva. A double cuticle covers the mouth (arrowhead). (C) Cherry detected in a coelomocyte (arrow) of a young adult. (D) MLT-10::mCherry found in strands (arrows) near the surface of a young adult. Scale bars, 10 μm.

We also examined the morphology of the longitudinal alae on the adult exoskeleton. The alae of wild-type adults were continuous, straight, and comprised of three ridges (n = 28). In contrast, in many *mlt-10(ok2581)* and *mlt-10(tm3331)* mutants, segments of the alae were broken, branched, or comprised of four ridges (Figure 8). The alae were malformed in 24% (n = 80) of *mlt-10(lof)* mutants. The alae were similarly malformed in 72% (n = 22) of *mlt-10(mg364)* animals and the majority of *mgEx699[mlt-10]* adults. Atypical sausage-shaped structures were observed on the surface of some *mlt-10(gof)* mutants (Figure 8F). Thus, both LOF and GOF mutations of *mlt-10* affect the morphology of the adult exoskeleton, which is synthesized during the final molt. Taken together, these ob-

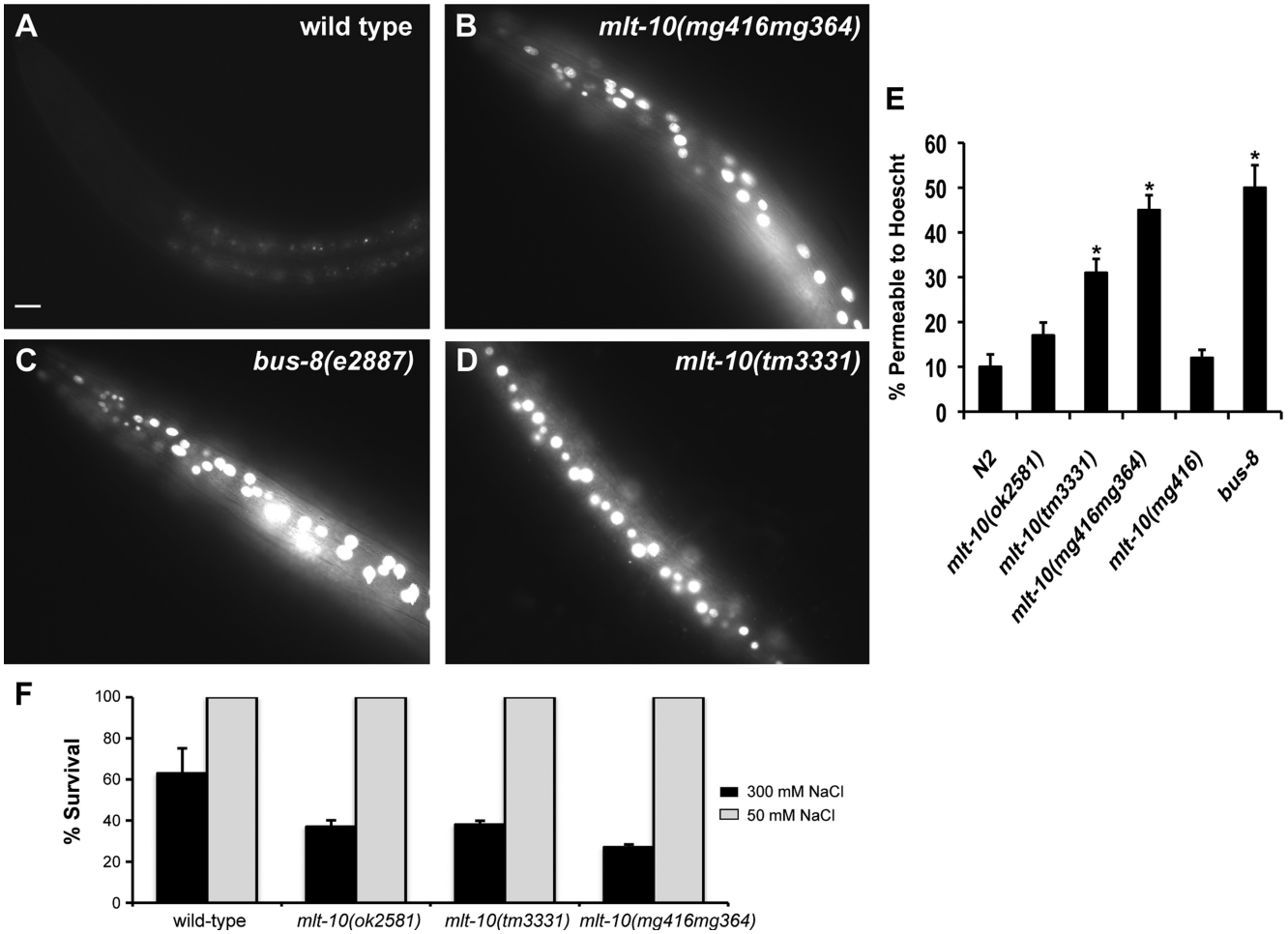

Figure 6. Increased permeability of the cuticle in *mlt-10* mutants. (A–D) Representative fluorescence micrographs of larvae stained with Hoechst 33258. All images were acquired with an exposure time of 50 ms. Scale bar, 10 μm. (E) The fraction of larvae with nuclei stained by Hoechst 33258. Values represent the average of two independent experiments; error bars, SEM. Asterisks indicate a significant difference from wild-type animals ($p \leq 0.05$). (F) Early L1 stage larvae of the indicated genotypes were collected and cultured on high-salt or standard NGM plates for 3 d at 20°C. Values represent the average of two independent experiments; error bars, SEM.

servations indicate that *mlt-10* is involved in the synthesis of new cuticles, as well as the removal of old ones.

Mutations of mlt-10 Affect Development of the Epidermis

Molting requires the coordinated activity of epidermal cells and syncytia spread across the body. We therefore examined the status of the epidermis in *mlt-10* mutants, focusing on the stem cell-like lateral seam cells, which produce the longitudinal alae. The seam cells divide asymmetrically early in the L1 stage (Soulston and Horvitz, 1977). Afterward, the anterior daughters fuse with the hypodermis, whereas the posterior daughters elongate and reconnect with one another. In this report, adherens junctions at the seam cell margins were detected using the AJM-1::GFP fusion protein and the seam cell nuclei were detected using a *scm::gfp* transcriptional fusion gene, as previously described (Hope, 1991; Mohler *et al.,* 1998). As expected, bilateral rows of rectangular cells were observed in wild-type larvae late in the L1 stage (Figure 9A; Podbilewicz and White, 1994). In contrast, particular seam cells were misshapen and overlapped their sisters in *mlt-10(tm3331)* and *mlt-10(ok2581)* mutants (Figure 9B). Abnormal cells were observed in 6% (n = 278) of *mlt-10(tm3331)* mutants, but were not observed in any of 150 wild-type larvae. Oddly shaped seam cells were also present in 8.5% (n = 200) of *mlt-10(mg416mg364)* larvae at this stage of development (Figure 9, C and D).

In wild-type animals, the seam cells fuse with their sisters late in the L4 stage and thereafter cease to divide (Soulston and Horvitz, 1977). The resulting bilateral syncytia were malformed and contained extra nuclei in some *mlt-10(mg416mg364)* mutants, a phenotype suggestive of seam cell hyperplasia (Figure 9F). Moreover, the syncytial seam of many *Ex[mlt-10::mCherry]* and *mlt-10(mg364)* adults contained gaps lacking detectable AJM-1 at the cell margins (Figure S6 and data not shown). In addition, GFP was detected outside of the syncytial seam in the majority of *mlt-10(lof)* and *mlt-10(416mg364)* mutants expressing the *scm::gfp* and *ajm-1::gfp* fusion genes (Figure 9H). Preliminary studies using Nomarski microscopy and DAPI staining identified some sites of ectopic GFP expression as hypodermal nucleoli. Collectively, these findings show that mutations of *mlt-10* affect several aspects of epidermal development, including dynamic changes in cell shape. Aberrant development of the seam cells likely contributes to the malformation of alae in *mlt-10* mutants and possibly to defects in the molting cycle.

We obtained additional information about the status of the seam cells in *mlt-10* mutants by staining larvae with the

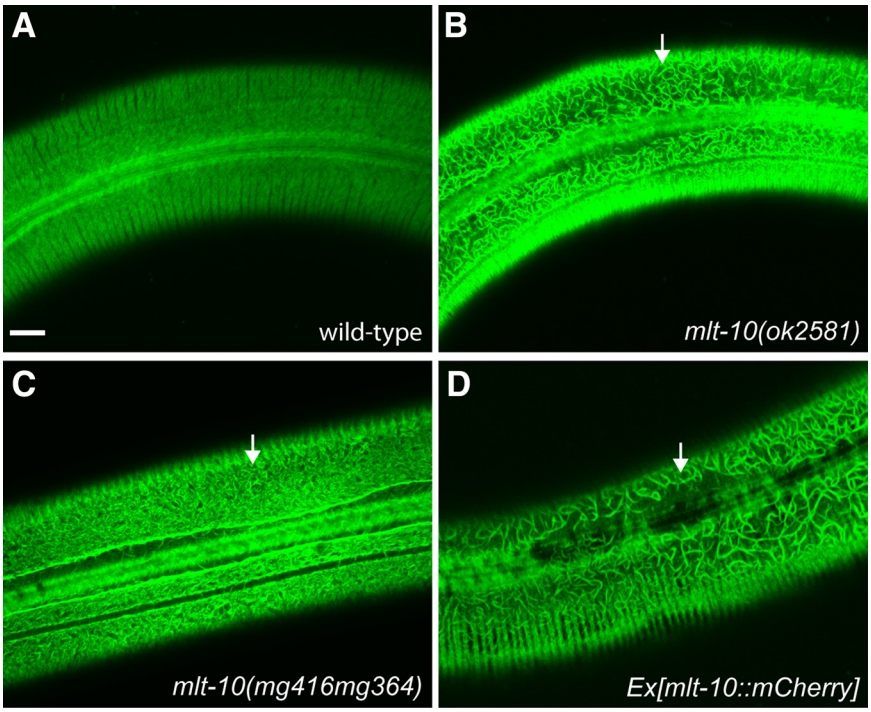

Figure 7. Disorganization of a cuticle collagen in *mlt-10* mutants. (A–D) Representative confocal fluorescence micrographs show COL-19::GFP in the adult exoskeleton. Arrows point to disorganized assemblies of COL-19::GFP flanking the longitudinal alae. Scale bar, 10 μm.

lectin wheat germ agglutinin (WGA) conjugated to the fluorescent dye Alexa Fluor 488 (Figure S7). Similar probes are regularly used to detect the surface glycans of *C. elegans* (Politz *et al.*, 1990), and mucin-type glycans are major ligands of WGA in this system (Natsuka *et al.*, 2005). WGA bound to the margins of the seam cells in *mlt-10(mg364)* mutants but not in wild-type larvae (Figure S7), suggesting the unnatural exposure or accretion of particular glycans. Those glycans may influence the adhesiveness and shape of the seam cells. Widespread ligands of WGA were also de-

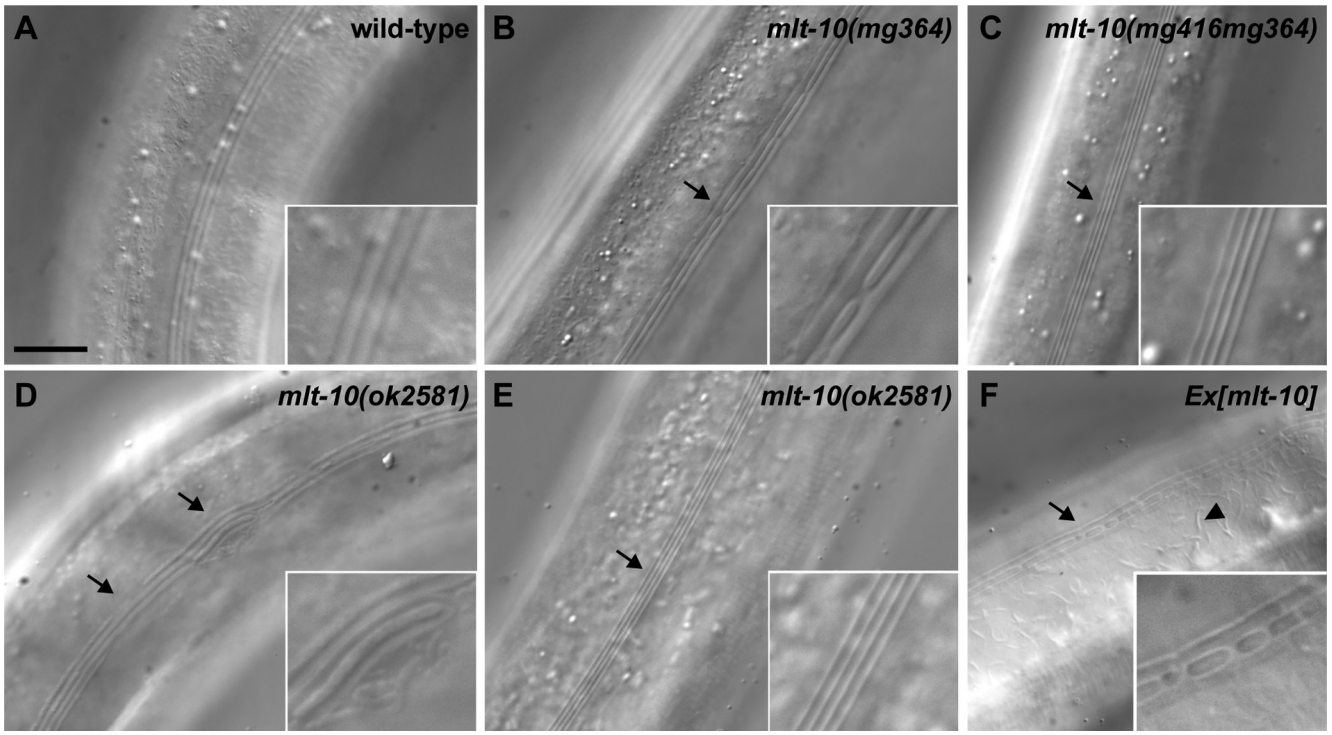

Figure 8. Malformation of the adult-specific alae in *mlt-10* mutants. (A–F) Representative Nomarski micrographs show the adult exoskeleton. Arrow, abnormalities in the alae including gaps, branches, and regions with four ridges. Arrowhead, an atypical structure in the cuticle. Each region of interest was digitally magnified 2.5-fold for display in the inset. Scale bar, 10 μm.

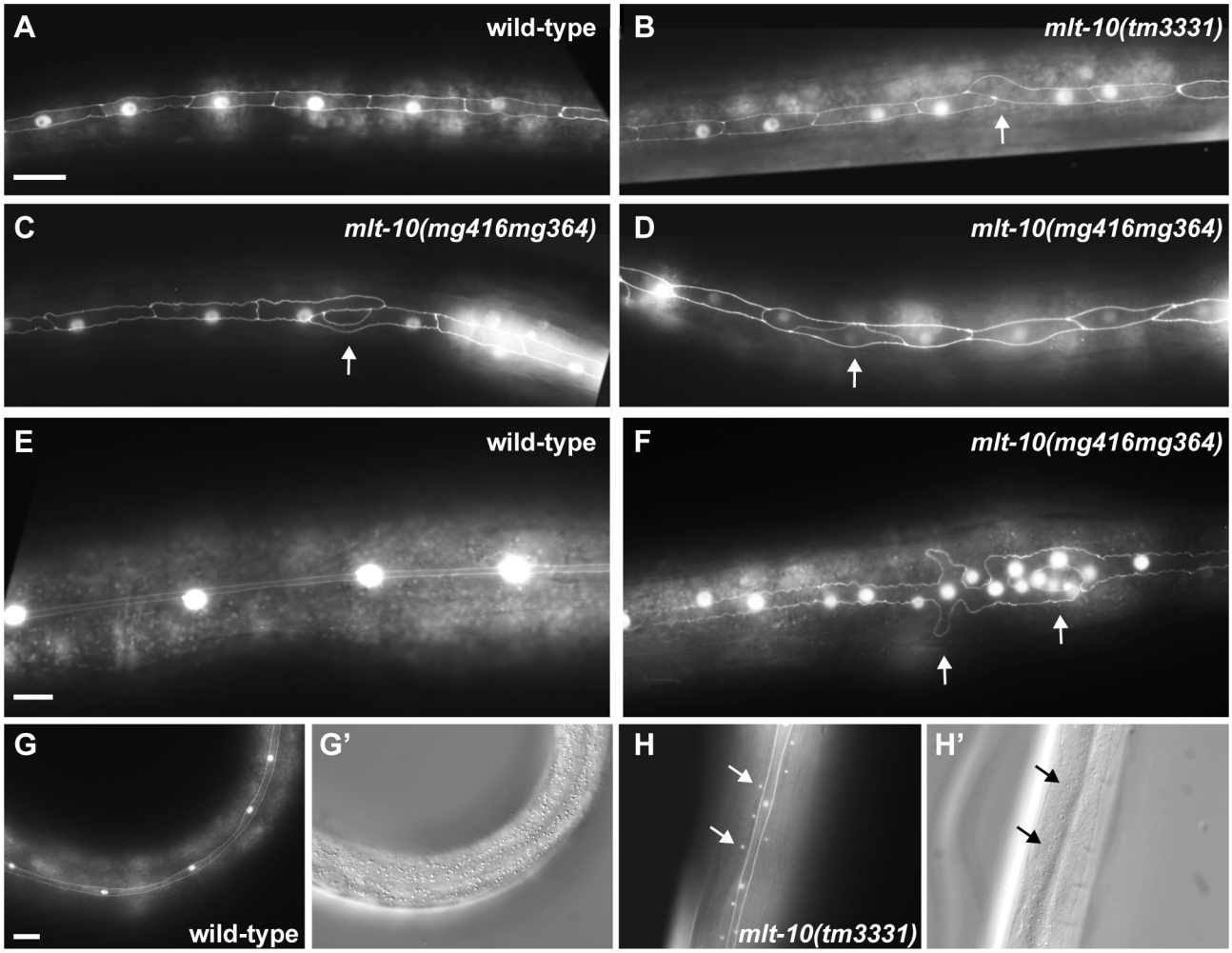

Figure 9. Abnormal development of the epidermis in *mlt-10* mutants. (A–F) Fluorescence micrographs show expression of AJM-1::GFP and the nuclear *scm::gfp* reporter in the lateral hypodermis. The anterior end of each worm is to the right, and the ventral side is down. All images were acquired with an exposure time of 500 ms. Scale bars, 10 μm. (A–D) Hatchlings were cultured on NGM for 16 h at 25°C before imaging. Arrows, irregularly shaped seam cells in the late L1 larvae. (E and F) Larvae were imaged late in the L4 stage. Arrows, an irregularly shaped region of the syncytial seam with extra nuclei. (G and H) Representative fluorescence and Nomarski micrographs show adults. Arrows, examples of GFP detected outside of the syncytial seam. Ectopic expression of GFP was observed in 80% (n = 54) of *mlt-10(tm3331)* mutants, 73% (n = 44) of *mlt-10(ok2581)* animals, and 81% (n = 114) of *mlt-10(mg416m364)* adults, but was not observed in wild-type animals (n = 36).

tected in the shed cuticles (molts) of *mlt-10* mutants and wild-type larvae. Moreover, ligands of WGA were concentrated at the anterior end of partly shed cuticles on *mlt-10(lof)* and *mlt-10(mg364)* mutants (Figure S7). Such mucus has not yet been observed on wild-type larvae, but could, in theory, provide natural lubrication at the moment of ecdysis.

Additional Phenotypes of mlt-10 Mutants

A variety of other phenotypes were associated with the *mlt-10(mg364)* mutation, including the presence of large, seemingly fluid-filled spaces and vacuoles in the body; aberrant shape of the body; uncoordinated movement; and improper development of the gonad and vulva. Some of these phenotypes may be attributable to abnormalities in the exoskeleton and epidermis. Notably, *mlt-10(mg364)* adults produced only 6 ± 10 (n = 18) progeny, whereas wild-type animals produced 262 ± 26 (n = 9) offspring. The cause of this sterility is not yet understood.

DISCUSSION

Here, we describe the isolation and characterization of the *mlt-10* gene of *C. elegans*. MLT-10 is the first reported member of a large family of nematode-specific proteins characterized by DUF644 and tandem P-X_2-L-(S/T)-P repeats. The *mg364* allele of *mlt-10* emerged from a genetic screen on low cholesterol. The mutation specifies the substitution H590Y in the repetitive region of MLT-10 and is thought to interfere with the function of multiple members of the MLT-10 family. Nine additional alleles of *mlt-10*, including two intragenic deletions and four substitution mutations, as well as high-copy *mlt-10* arrays, were used to analyze the role of *mlt-10* in larval development.

Our findings suggest that MLT-10 is a secreted protein involved in the removal of old cuticles as well as the synthesis of new cuticles. In review, either the loss or the gain of *mlt-10* function impedes the shedding of old cuticles. Both LOF and GOF mutations of *mlt-10* are also associated with abnormalities in the larval and adult exoskeletons. The syn-

thesis and removal of cuticles are almost certainly interconnected in nematodes, as newly synthesized cuticles displace the preexisting ones during the process of molting. Consistent with that view, deformities in the ultrastructure of the underlying cuticle have been observed in particular molting-defective mutants (Hao *et al.*, 2006). Moreover, certain enzymes involved in the biosynthesis of collagens and other ECM proteins are needed for the removal of larval cuticles, including the glycosyltransferase BUS-8, the peroxidases BLI-3 and MLT-7, and the protease BLI-5 (Edens *et al.*, 2001; Davis *et al.*, 2004; Frand *et al.*, 2005; Page *et al.*, 2006; Partridge *et al.*, 2008; Thein *et al.*, 2009; Stepek *et al.*, 2010). In theory, progress through ecdysis might depend on physiological feedback on the status of the new exoskeleton. Consistent with that idea, animals forced to ecdyse before completion of a new cuticle perish, probably due to osmotic shock (Ruaud and Bessereau, 2006).

Mutations of *mlt-10* also affect the development of epidermal cells and syncytia that synthesize the exoskeleton. Notably, several transcription factors required for proper development of the seam cells are also necessary to remove larval cuticles, including NHR-25 and the GATA factors ELT-5 and -6 (Asahina *et al.*, 2000; Gissendanner and Sluder, 2000; Koh and Rothman, 2001; Chen *et al.*, 2004; Silhankova *et al.*, 2005). We hypothesize that some abnormalities in seam cell development observed in *nhr-25* mutants relate to the deregulation of *mlt-10.* Further, we speculate that MLT-10 directly or indirectly affects cell–ECM interactions important for epidermal development.

Using a transcriptional fusion gene, we show that *mlt-10* is transiently expressed in hypodermal cells and syncytia whenever the exoskeleton is remade. The conserved nuclear hormone receptors NHR-23 and -25 are required for the periodic expression of *mlt-10*. Consequently, the amount of *mlt-10* expressed at any time in development probably relates to the abundance of steroid hormones that bind these receptors. Transcriptional control by NHR-23 and -25 may coordinate the expression of MLT-10 with the production of particular collagens, matrix modification enzymes, and signaling molecules involved in the molting cycle.

Two full-length, translational fusion proteins were used to evaluate the distribution of MLT-10. Both the MLT-10::mCherry and the GFP::MLT-10 fusion proteins were detected in putative vesicles in the lateral hypodermis during molting. The MLT-10::mCherry fusion protein was also detected in strands near the surface of animals. After completion of the molting cycle, Cherry was detected in coelomocytes. Collectively, these findings suggest that MLT-10 is secreted from the hypodermis to the surrounding matrices and fluids during the process of molting.

Proline-rich repeats are found in several well-characterized extracellular proteins, including collagen, elastin, and flagelliform silks (Bhattacharjee and Bansal, 2005; He *et al.*, 2007; Matsushima *et al.*, 2008; Savage and Gosline, 2008; Wise and Weiss, 2009). After comparing MLT-10 with these proteins, we predict that three main factors contribute to the secondary structure of the C-terminal region of MLT-10: 1) steric repulsion among proline residues, 2) attraction among hydrophobic residues, and 3) hydrogen bonding among hydroxy amino acids. One possibility is that the P-X_2-L-(S/T)-P repeats of MLT-10 promote the assembly of oligomeric complexes, perhaps including other MLTN proteins. The structure of any such complexes would likely be distinct from collagen, because the P-X_2-L-(S/T)-P repeats contain very few glycine residues. An alternative possibility is that the C-terminal region of MLT-10 lacks regular secondary structure and mostly provides extension or flexibility. In either case, we expect the tertiary structure of MLT-10 to allow segregation of the hydrophobic P-X_2-L-(S/T)-P repeats from the hydrophilic DUF644.

We propose that the molting cycle involves the dynamic assembly and disassembly of oligomeric MLT-10 complexes. In principle, the MLT-10(H590Y) substitution mutation might interfere with intermolecular interactions among multiple members of the MLTN family, by altering the electrochemical properties of the repetitive region or forming inappropriate di-tyrosine cross-links. Interference with multiple paralogs could account for the severe phenotypes caused by the *mlt-10(mg364)* mutation. Excessive production of MLT-10 might also disrupt interactions between MLT-10 and the MLTN proteins. Notably, many disease-associated substitution mutations in human collagens interfere with the assembly of collagen fibrils (Blank and Boskey, 2008). Studies of these particular dominant-negative mutations in collagens have greatly enriched our understanding of ECM remodeling in human development and disease.

Our working model is that MLT-10 serves as an instructive or structural component of the cuticle and thereby influences the assembly or disassembly of collagens. Alternatively, MLT-10 might promote the trafficking of collagens through the secretory pathway of the hypodermis. A similar function has been proposed for the membrane-spanning proteins CUTI-1 and TSP-15, which are required for shedding larval cuticles (Moribe *et al.*, 2004; Fritz and Behm, 2009). A third possibility is that MLT-10 and the paralogs of MLT-10 serve as monomeric lubricants that help dislodge old cuticles from the hypodermis. As lubricants, the MLTN proteins might also facilitate particular behaviors used to escape old cuticles, including longitudinal rotation. Further research is needed to fully define the function of MLT-10.

The increased dependence of *mlt-10* mutants on exogenous cholesterol suggests a reduced capacity to acquire or utilize sterols. We therefore speculate that mutations of *mlt-10* directly or indirectly reduce the function of other proteins linked to sterols and essential for shedding cuticles. Those proteins include the hedgehog-like protein QUA-1, several homologues of Patched, and the low-density lipoprotein receptor-like protein LRP-1 (Yochem *et al.*, 1999; Zugasti *et al.*, 2005; Hao *et al.*, 2006). LRP-1 is expressed on the apical surface of the hypodermis (Yochem *et al.*, 1999), which may represent an important site of sterol uptake in nematodes (Fleming and Fetterer, 1984).

Our ongoing investigation of the MLT-10 family may directly benefit the development of new drugs for filarial diseases currently affecting over 140 million people living primarily in tropical regions. The compounds currently in use target ion channels and cytoskeletal proteins that are conserved between nematodes and mammals, and these compounds can be toxic to humans. In contrast, DUF644 is well conserved only in nematodes. Surface glycoproteins also comprise major antigens of parasitic nematodes (Blaxter *et al.*, 1992) and may include multiple homologues of MLT-10. The homologues of MLT-10 are therefore attractive targets for drug development.

ACKNOWLEDGMENTS

We thank Julie Ahringer and Marc Vidal for providing bacterial clones. We are grateful to Chris Miller, David Eisenberg, Robert Mecham, Fred Keeley, and Creg Darby for helpful discussions. We thank John Kim, Peter Edwards, and Stanford Frand for critical reading of the manuscript. We thank the *C. elegans* Knockout Consortium, Shohei Mitani of the Tokyo Women's Medical University, and Laurent Segalat for providing additional strains. This work was supported by funds from the David Geffen School of Medicine at UCLA; postdoctoral fellowships from the Jane Coffin Childs Memorial Foundation

and the MGH Fund for Medical Discovery to A.F.; and a National Institutes of Health grant to G.R. Some strains used in this study were provided by the *Caenorhabditis* Genetics Center (CGC).

REFERENCES

Aguinaldo, A. M., Turbeville, J. M., Linford, L. S., Rivera, M. C., Garey, J. R., Raff, R. A., and Lake, J. A. (1997). Evidence for a clade of nematodes, arthropods and other moulting animals. Nature *387*, 489–493.

Altschul, S. F., Gish, W., Miller, W., Myers, E. W., and Lipman, D. J. (1990). Basic local alignment search tool. J. Mol. Biol. *215*, 403–410.

Asahina, M., Ishihara, T., Jindra, M., Kohara, Y., Katsura, I., and Hirose, S. (2000). The conserved nuclear receptor Ftz-F1 is required for embryogenesis, moulting and reproduction in *Caenorhabditis elegans*. Genes Cells *5*, 711–723.

Bessereau, J. L., Wright, A., Williams, D. C., Schuske, K., Davis, M. W., and Jorgensen, E. M. (2001). Mobilization of a *Drosophila* transposon in the *Caenorhabditis elegans* germ line. Nature *413*, 70–74.

Bhattacharjee, A., and Bansal, M. (2005). Collagen structure: the Madras triple helix and the current scenario. IUBMB Life *57*, 161–172.

Blank, R. D., and Boskey, A. L. (2008). Genetic collagen diseases: influences of collagen mutations on structure and mechanical behavior. In: Collagen: Structure and Mechanics, ed. P. Fratzl, New York: Springer Science, 447–464.

Blaxter, M. L., Page, A. P., Rudin, W., and Maizels, R. M. (1992). Nematode surface coats: actively evading immunity. Parasitol. Today *8*, 243–247.

Campbell, K. P. (1995). Three muscular dystrophies: loss of cytoskeleton-extracellular matrix linkage. Cell *80*, 675–679.

Chen, Z., Eastburn, D. J., and Han, M. (2004). The *Caenorhabditis elegans* nuclear receptor gene nhr-25 regulates epidermal cell development. Mol. Cell. Biol. *24*, 7345–7358.

Chitwood, D. J. (1999). Biochemistry and function of nematode steroids. Crit. Rev. Biochem. Mol. Biol. *34*, 273–284.

Cox, G. N., Kusch, M., and Edgar, R. S. (1981). Cuticle of *Caenorhabditis elegans*: its isolation and partial characterization. J. Cell Biol. *90*, 7–17.

Crowder, C. M., Westover, E. J., Kumar, A. S., Ostlund, R. E., Jr., and Covey, D. F. (2001). Enantiospecificity of cholesterol function in vivo. J. Biol. Chem. *276*, 44369–44372.

Davis, M. W., Birnie, A. J., Chan, A. C., Page, A. P., and Jorgensen, E. M. (2004). A conserved metalloprotease mediates ecdysis in *Caenorhabditis elegans*. Development *131*, 6001–6008.

Edens, W. A., *et al.* (2001). Tyrosine cross-linking of extracellular matrix is catalyzed by Duox, a multidomain oxidase/peroxidase with homology to the phagocyte oxidase subunit gp91phox. J. Cell Biol. *154*, 879–891.

Emsley, P., Charles, I. G., Fairweather, N. F., and Isaacs, N. W. (1996). Structure of *Bordetella* pertussis virulence factor P.69 pertactin. Nature *381*, 90–92.

Epstein, H. F., and Shakes, D. C. (eds.) (1995). *Caenorhabditis elegans*: Modern Biological Analysis of an Organism, San Diego: Academic Press.

Fetterer, R. H., and Rhoads, M. L. (1990). Tyrosine-derived cross-linking amino acids in the sheath of *Haemonchus contortus* infective larvae. J. Parasitol. *76*, 619–624.

Fleming, M. W., and Fetterer, R. H. (1984). *Ascaris suum*: continuous perfusion of the pseudocoelom and nutrient absorption. Exp. Parasitol. *57*, 142–148.

Frand, A. R., Russel, S., and Ruvkun, G. (2005). Functional genomic analysis of *C. elegans* molting. PLoS Biol. *3*, e312.

Fraser, A. G., Kamath, R. S., Zipperlen, P., Martinez-Campos, M., Sohrmann, M., and Ahringer, J. (2000). Functional genomic analysis of *C. elegans* chromosome I by systematic RNA interference. Nature *408*, 325–330.

Fritz, J. A., and Behm, C. A. (2009). CUTI-1, a novel tetraspan protein involved in *C. elegans* CUTicle formation and epithelial integrity. PLoS One *4*, e5117.

Gissendanner, C. R., and Sluder, A. E. (2000). nhr-25, the *Caenorhabditis elegans* ortholog of ftz-f1, is required for epidermal and somatic gonad development. Dev. Biol. *221*, 259–272.

Grant, B. D., and Sato, M. (2006). Intracellular trafficking (January 21, 2006), *WormBook*, ed. The *C. elegans* Research Community, WormBook, doi/10.1895/wormbook.1.77.1, http://www.wormbook.org.

Hao, L., Mukherjee, K., Liegeois, S., Baillie, D., Labouesse, M., and Burglin, T. R. (2006). The hedgehog-related gene qua-1 is required for molting in *Caenorhabditis elegans*. Dev. Dyn. *235*, 1469–1481.

Hashmi, S., Britton, C., Liu, J., Guiliano, D. B., Oksov, Y., and Lustigman, S. (2002). Cathepsin L is essential for embryogenesis and development of *Caenorhabditis elegans*. J. Biol. Chem. 277, 3477–3486.

Hashmi. S., Zhang, J., Oksov, Y., and Lustigman, S. (2004). The *Caenorhabditis elegans* cathepsin Z-like cysteine protease, Ce-CPZ-1, has a multifunctional role during the worms' development. J. Biol. Chem. 279, 6035–6045.

Hayes, G. D., Frand, A. R., and Ruvkun, G. (2006). The mir-84 and let-7 paralogous microRNA genes of *Caenorhabditis elegans* direct the cessation of molting via the conserved nuclear hormone receptors NHR-23 and NHR-25. Development *133*, 4631–4641.

He, D., Chung, M., Chan, E., Alleyne, T., Ha, K. C., Miao, M., Stahl, R. J., Keeley, F. W., and Parkinson, J. (2007). Comparative genomics of elastin: sequence analysis of a highly repetitive protein. Matrix Biol. *26*, 524–540.

Hieb, W., and Rothstein, M. (1968). Sterol requirement for reproduction of a free-living nematode. Science *160*, 778–780.

Hope, I. A. (1991). 'Promoter trapping' in *Caenorhabditis elegans*. Development *113*, 399–408.

Johnstone, I. L. (1994). The cuticle of the nematode *Caenorhabditis elegans*: a complex collagen structure. Bioessays *16*, 171–178.

Kamath, R. S., *et al.* (2003). Systematic functional analysis of the *Caenorhabditis elegans* genome using RNAi. Nature *421*, 231–237.

Koh, K., and Rothman, J. H. (2001). ELT-5 and ELT-6 are required continuously to regulate epidermal seam cell differentiation and cell fusion in *C. elegans*. Development *128*, 2867–2880.

Kostrouchova, M., Krause, M., Kostrouch, Z., and Rall, J. E. (1998). CHR3, a *Caenorhabditis elegans* orphan nuclear hormone receptor required for proper epidermal development and molting. Development *125*, 1617–1626.

Kostrouchova, M., Krause, M., Kostrouch, Z., and Rall, J. E. (2001). Nuclear hormone receptor CHR3 is a critical regulator of all four larval molts of the nematode *Caenorhabditis elegans*. Proc. Natl. Acad. Sci. USA *98*, 7360–7365.

Krause, K., and Foitzik, K. (2006). Biology of the hair follicle: the basics. Semin. Cutan. Med. Surg. *25*, 2–10.

Li, J., Brown, G., Ailion, M., Lee, S., and Thomas, J. H. (2004). NCR-1 and NCR-2, the *C. elegans* homologs of the human Niemann-Pick type C1 disease protein, function upstream of DAF-9 in the dauer formation pathways. Development *131*, 5741–5752.

Li, X., Zhao, X., Fang, Y., Jiang, X., Duong, T., Fan, C., Huang, C. C., and Kain, S. R. (1998). Generation of destabilized green fluorescent protein as a transcription reporter. J. Biol. Chem. *273*, 34970–34975.

Lustigman, S., Brotman, B., Huima, T., Castelhano, A. L., Singh, R. N., Mehta, K., and Prince, A. M. (1995). Transglutaminase-catalyzed reaction is important for molting of *Onchocerca volvulus* third-stage larvae. Antimicrob. Agents Chemother. *39*, 1913–1919.

Martin, E., Laloux, H., Couette, G., Alvarez, T., Bessou, C., Hauser, O., Sookhareea, S., Labouesse, M., and Segalat, L. (2002). Identification of 1088 new transposon insertions of *Caenorhabditis elegans*: a pilot study toward large-scale screens. Genetics *162*, 521–524.

Matsushima, N., Yoshida, H., Kumaki, Y., Kamiya, M., Tanaka, T., Izumi, Y., and Kretsinger, R. H. (2008). Flexible structures and ligand interactions of tandem repeats consisting of proline, glycine, asparagine, serine, and/or threonine rich oligopeptides in proteins. Curr. Protein Pept. Sci. *9*, 591–610.

Matyash, V., Entchev, E. V., Mende, F., Wilsch-Brauninger, M., Thiele, C., Schmidt, A. W., Knolker, H. J., Ward, S., and Kurzchalia, T. V. (2004). Sterol-derived hormone(s) controls entry into diapause in *Caenorhabditis elegans* by consecutive activation of DAF-12 and DAF-16. PLoS Biol. *2*, e280.

Merris, M., Wadsworth, W. G., Khamrai, U., Bittman, R., Chitwood, D. J., and Lenard, J. (2003). Sterol effects and sites of sterol accumulation in *Caenorhabditis elegans*: developmental requirement for 4alpha-methyl sterols. J. Lipid Res. *44*, 172–181.

Mohler, W. A., Simske, J. S., Williams-Masson, E. M., Hardin, J. D., and White, J. G. (1998). Dynamics and ultrastructure of developmental cell fusions in the *Caenorhabditis elegans* hypodermis. Curr. Biol. *8*, 1087–1090.

Moribe, H., Yochem, J., Yamada, H., Tabuse, Y., Fujimoto, T., and Mekada, E. (2004). Tetraspanin protein (TSP-15) is required for epidermal integrity in *Caenorhabditis elegans*. J. Cell Sci. *117*, 5209–5220.

Motola, D. L., *et al.* (2006). Identification of ligands for DAF-12 that govern dauer formation and reproduction in *C. elegans*. Cell *124*, 1209–1223.

Natsuka, S., Kawaguchi, M., Wada, Y., Ichikawa, A., Ikura, K., and Hase, S. (2005). Characterization of wheat germ agglutinin ligand on soluble glycoproteins in *Caenorhabditis elegans*. J. Biochem. *138*, 209–213.

Page, A. P., and Johnstone, I. L. The cuticle (March 19, 2007), *WormBook*, ed. The *C. elegans* Research Community, WormBook, doi/10.1895/wormbook.1.138.1, http://www.wormbook.org.

Page, A. P., McCormack, G., and Birnie, A. J. (2006). Biosynthesis and enzymology of the *Caenorhabditis elegans* cuticle: identification and characterization of a novel serine protease inhibitor. Int. J. Parasitol. *36*, 681–689.

Page-McCaw, A., Ewald, A. J., and Werb, Z. (2007). Matrix metalloproteinases and the regulation of tissue remodelling. Nat. Rev. Mol. Cell Biol. *8*, 221–233.

Partridge, F. A., Tearle, A. W., Gravato-Nobre, M. J., Schafer, W. R., and Hodgkin, J. (2008). The *C. elegans* glycosyltransferase BUS-8 has two distinct and essential roles in epidermal morphogenesis. Dev. Biol. *317*, 549–559.

Pasquinelli, A. E., *et al.* (2000). Conservation of the sequence and temporal expression of let-7 heterochronic regulatory RNA. Nature *408*, 86–89.

Podbilewicz, B., and White, J. G. (1994). Cell fusions in the developing epithelial of *C. elegans*. Dev. Biol. *161*, 408–424.

Politz, S. M., Philipp, M., Estevez, M., O'Brien, P. J., and Chin, K. J. (1990). Genes that can be mutated to unmask hidden antigenic determinants in the cuticle of the nematode *Caenorhabditis elegans*. Proc. Natl. Acad. Sci. USA *87*, 2901–2905.

Ramirez, F., and Dietz, H. C. (2009). Extracellular microfibrils in vertebrate development and disease processes. J. Biol. Chem. *284*, 14677–14681.

Roberts, B., Clucas, C., and Johnstone, I. L. (2003). Loss of SEC-23 in *Caenorhabditis elegans* causes defects in oogenesis, morphogenesis, and ECM secretion. Mol. Biol. Cell 14, 4414–4426.

Roudier, N., Lefebvre, C., and Legouis, R. (2005). CeVPS-27 is an endosomal protein required for the molting and the endocytic trafficking of the low-density lipoprotein receptor-related protein 1 in *Caenorhabditis elegans*. Traffic *6*, 695–705.

Ruaud, A. F., and Bessereau, J. L. (2006). Activation of nicotinic receptors uncouples a developmental timer from the molting timer in *C. elegans*. Development *133*, 2211–2222.

Ruaud, A. F., Lam, G., and Thummel, C. S. (2010). The *Drosophila* nuclear receptors DHR3 and betaFTZ-F1 control overlapping developmental responses in late embryos. Development *137*, 123–131.

Sapio, M. R., Hilliard, M. A., Cermola, M., Favre, R., and Bazzicalupo, P. (2005). The Zona Pellucida domain containing proteins, CUT-1, CUT-3 and CUT-5, play essential roles in the development of the larval alae in *Caenorhabditis elegans*. Dev. Biol. *282*, 231–245.

Savage, K. N., and Gosline, J. M. (2008). The role of proline in the elastic mechanism of hydrated spider silks. J. Exp. Biol. *211*, 1948–1957.

Silhankova, M., Jindra, M., and Asahina, M. (2005). Nuclear receptor NHR-25 is required for cell-shape dynamics during epidermal differentiation in *Caenorhabditis elegans*. J. Cell Sci. *118*, 223–232.

Simmer, F., Tijsterman, M., Parrish, S., Koushika, S. P., Nonet, M. L., Fire, A., Ahringer, J., and Plasterk, R. H. (2002). Loss of the putative RNA-directed RNA polymerase RRF-3 makes *C. elegans* hypersensitive to RNAi. Curr. Biol. *12*, 1317–1319.

Singh, R. N., and Soulston, J. E. (1978). Some observations on moulting in *Caenorhabditis elegans*. Nematologica *24*, 63–71.

Smith, M. M., and Levitan, D. J. (2007). Human NPC1L1 and NPC1 can functionally substitute for the ncr genes to promote reproductive development in *C. elegans*. Biochim. Biophys. Acta *1770*, 1345–1351.

Soulston, J. E., and Horvitz, H. R. (1977). Post-embryonic cell lineages of the nematode, *Caenorhabditis elegans*. Dev. Biol. *56*, 110–156.

Stepek, G., McCormack, G., and Page, A. P. (2010). The kunitz domain protein BLI-5 plays a functionally conserved role in cuticle formation in a diverse range of nematodes. Mol. Biochem. Parasitol. *169*, 1–11.

Suzuki, M., Sagoh, N., Iwasaki, H., Inoue, H., and Takahashi, K. (2004). Metalloproteases with EGF, CUB, and thrombospondin-1 domains function in molting of *Caenorhabditis elegans*. Biol. Chem. *385*, 565–568.

Sym, M., Basson, M., and Johnson, C. (2000). A model for niemann-pick type C disease in the nematode *Caenorhabditis elegans*. Curr. Biol. *10*, 527–530.

Thacker, C., and Rose, A. M. (2000). A look at the *Caenorhabditis elegans* Kex2/Subtilisin-like proprotein convertase family. Bioessays *22*, 545–553.

Thein, M. C., McCormack, G., Winter, A. D., Johnstone, I. L., Shoemaker, C. B., and Page, A. P. (2003). *Caenorhabditis elegans* exoskeleton collagen COL-19, an adult-specific marker for collagen modification and assembly, and the analysis of organismal morphology. Dev. Dyn. *226*, 523–539.

Thein, M. C., Winter, A. D., Stepek, G., McCormack, G., Stapleton, G., Johnstone, I. L., and Page, A. P. (2009). Combined extracellular matrix cross-linking activity of the peroxidase MLT-7 and the dual oxidase BLI-3 is critical for post-embryonic viability in *Caenorhabditis elegans*. J. Biol. Chem. *284*, 17549–17563.

Thummel, C. S. (1996). Files on steroids—*Drosophila* metamorphosis and the mechanisms of steroid hormone action. Trends Genet. *12*, 306–310.

Timmons, L., Court, D. L., and Fire, A. (2001). Ingestion of bacterially expressed dsRNAs can produce specific and potent genetic interference in *Caenorhabditis elegans*. Gene *263*, 103–112.

Wicks, S. R., Yeh, R. T., Gish, W. R., Waterston, R. H., and Plasterk, R. H. (2001). Rapid gene mapping in *Caenorhabditis elegans* using a high density polymorphism map. Nat. Genet. *28*, 160–164.

Wise, S. G., and Weiss, A. S. (2009). Tropoelastin. Int. J. Biochem. Cell Biol. *41*, 494–497.

Yochem, J., Gu, T., and Han, M. (1998). A new marker for mosaic analysis in *Caenorhabditis elegans* indicates a fusion between hyp6 and hyp7, two major components of the hypodermis. Genetics *149*, 1323–1334.

Yochem, J., Tuck, S., Greenwald, I., and Han, M. (1999). A gp330/megalin-related protein is required in the major epidermis of *Caenorhabditis elegans* for completion of molting. Development *126*, 597–606.

Zugasti, O., Rajan, J., and Kuwabara, P. E. (2005). The function and expansion of the Patched- and Hedgehog-related homologs in *C. elegans*. Genome Res. *15*, 1402–1410.